

## Supporting Information

# Methane Pyrolysis Byproduct Challenge: Carbon Black Absorption by Calcium Carbide Manufacturing

Dmitriy E. Samoylenko,<sup>a</sup> Konstantin I. Dement'ev,<sup>b</sup> Anton L. Maksimov,<sup>b</sup> and Konstantin S. Rodygin\*<sup>a</sup>

<sup>[a]</sup> Institute of Chemistry, Saint Petersburg State University, 7/9 Universitetskaya nab., St. Petersburg, 199034, Russia.

<sup>[b]</sup> A.V. Topchiev Institute of Petrochemical Synthesis, Russian Academy of Sciences, Leninsky pr. 29, Moscow 119991, Russia.

Correspondence: [k.rodygin@spbu.ru](mailto:k.rodygin@spbu.ru)

## Contents

1. Materials and methods.....	2
2. The sensitivity of the analysis for gaseous products by components.....	4
3. Catalyst characterization .....	7
4. Analysis of the obtained carbon .....	13
5. NMR Spectra.....	16
6. EDX analysis of carbon sample.....	20
7. ICP data.....	26

## 1. Materials and methods

**General information.** Calcium carbide (granulated, particle size 0.1-1 mm, 75% of acetylene, gas-volumetric as indicated by the supplier), thiols, alcohols, amines and azides were purchased from Panreac, Alfa Aesar and abcr GmbH&Co, and used as received.

$^1\text{H}$  spectra were recorded using a Bruker Avance 400 NMR spectrometer. The  $^1\text{H}$  chemical shifts were reported in ppm and were determined using the signals of the residual solvent peaks. The data were processed using MestReNova software (version 6.0.2).

XRD data were collected using a Bruker "D2 Phaser" powder diffractometer operating with X-ray tube radiation -  $\text{CuK}\alpha_{1+2}$ , wavelengths  $\lambda_{\text{CuK}\alpha 1} = 1.54059 \text{ \AA}$  and  $\lambda_{\text{CuK}\alpha 2} = 1.54443 \text{ \AA}$ , tube operation mode 30 kV/10 mA, position-sensitive detector, reflection geometry, Bragg-Brentano focusing scheme, sample rotation speed 20 rpm, diffraction angle interval  $2\theta = 5(6.8)\text{-}90^\circ$ , scanning step  $0.02^\circ$ , exposure at a point 0.7 seconds,  $T=25^\circ\text{C}$ , atmosphere – air.

The surface of the carbon samples was investigated on a Zeiss Merlin SEM. EDX measurement were performed at 20 kV of accelerating voltage with the Oxford Instruments INCA X-Act spectrometer mounted on Zeiss Merlin SEM.

### Experimental

**The synthesis of the catalyst.** The synthesis of a catalyst was carried out by pH-controlled coprecipitation from solutions of metal nitrates with a total concentration of Mg, Al, and Ni cations of 1.0 mol/L. A solution of NaOH and  $\text{Na}_2\text{CO}_3$  with concentrations of 2.0 and 0.20 mol/L, respectively, was used as a precipitant. After coprecipitation, the precipitate was aged for 24 h. Then, the precipitate was washed and filtered under vacuum until the wash water reacted negatively to nitrate ions. The washed precipitate was dried at  $100\text{-}120^\circ\text{C}$  to constant weight. Then, thermolysis of the resulting hydrotalcite was carried out at a temperature of  $550^\circ\text{C}$ . In the second stage, the thermolysis products were placed into a  $\text{Na}_2[\text{Ni-EDTA}]$  solution and kept for 10 h. The resulting Ni-EDTA precipitate was washed and filtered under vacuum until the wash water became colourless. The washed precipitate was dried at  $100\text{-}120^\circ\text{C}$  to constant weight. The average particle size of the catalyst was  $150\text{-}200 \mu\text{m}$ .

**Catalytic test description.** Catalytic tests were carried out with a plug-flow quartz reactor. Then,  $2 \text{ cm}^3$  of quartz was loaded into the reactor as a substrate,  $2 \text{ cm}^3$  of the catalyst was loaded from above, and the hot junction of the thermocouple was placed directly in the catalyst layer. Before the experiment, the catalyst was activated for 2 h at  $420^\circ\text{C}$ . After activation, the start temperature ( $550^\circ\text{C}$ ) was set in the reactor, and methane was added. The experiment was carried out in the same mode for all catalysts. Relative space velocity  $2000 \text{ h}^{-1}$ . The temperature was changed automatically according to the following program: exposure for 30 min and heating for 3 min with a step of  $50^\circ\text{C}$ . Gas sampling for analysis was carried out three times for each mode 10, 20, and 30 min after the start.

After the reaction, the catalyst mixed with carbon black was treated with hydrochloric acid to remove the catalyst, after which the carbon black particles were filtered off, washed with distilled water and acetone, and dried.

**General Procedure for Pyrolysis of Methane and Analysis of the Products.** Feed and product gas analysis. The analysis of the gas product was carried out on a Crystallux-4000M chromatograph equipped with three columns and FID/TCD/TCD detector assembly. Nitrogen, carbon monoxide and hydrogen were determined on a packed column with a CaX molecular sieves ( $3 \text{ m} \times 3 \text{ mm}$ ), carbon dioxide was determined on a Porapak Q column ( $3 \text{ m} \times 3 \text{ mm}$ ), and  $\text{C}_1\text{-C}_6$  hydrocarbons were determined on an HP-Plot  $\text{Al}_2\text{O}_3/\text{Na}_2\text{SO}_4$  capillary column (Agilent,  $50 \text{ m}$ ,  $0.32 \text{ mm}$ ). The sensitivity of the analysis for gaseous products by components is given in Table S1.

**The general procedure for the synthesis of calcium carbide.** A mixture residue after pyrolysis of methane gas with calcium metal was loaded into a quartz tube and placed into an oven under an inert atmosphere. The oven was heated to 1100 °C for an hour. After the reaction, the oven was cooled to rt, and the residue was placed in a sealed vial and then used. The yield of the carbide was determined gravimetrically. The identity of acetylene gas released after the hydrolysis of carbide was determined using gas chromatography and an appropriate column. Simple volumetry was used to determine the yield of carbide and its purity. Note that the synthesized carbide is a black powder that is highly active and ready to hydrolyse.

Activated carbon, glassy carbon and charcoal were tested in the synthesis of calcium carbide to check the approach. As a result, calcium carbide was obtained in 93%, 66% and 92% yield for activated carbon, glassy carbon and charcoal, respectively.

**The procedure for burning of carbon residue.** A sample of solid residue after the pyrolysis of methane gas was placed into a thermogravimetric analyzer and heated under an oxygen atmosphere. Then, the weight loss was tracked during heating. Thus, the available carbon was burnt, and a non-flammable residue was formed.

**Volumetric determination of calcium carbide yield.** A round bottom flask equipped with a pressure-compensated dropping funnel and an outlet was charged with 25 mg of synthesized  $\text{CaC}_2$ . 25 ml of water was placed into a dropping funnel and sealed with a stopper. A silicone hose was connected to the outlet of the flask, the end of which was placed under water in an inverted 10 ml cylinder completely filled with water. Then, while stirring, water was added dropwise to the flask to ensure full hydrolysis, while acetylene was quickly released, the excess of which went through a hose into a graduated cylinder, which was used to determine the volume of the gas. Note that acetylene is very poorly soluble in water.

## 2. The sensitivity of the analysis for gaseous products by components

**Table S1.** Determination threshold of gaseous product analysis.

Component	Determination threshold, ppmv
H <sub>2</sub> , hydrogen	116
O <sub>2</sub> , oxygen	1170
N <sub>2</sub> , nitrogen	1330
CO, carbon monoxide	1380
CO <sub>2</sub> , carbon dioxide	1050
CH <sub>4</sub> , methane	26.5
C <sub>2</sub> hydrocarbons	13.5
C <sub>3</sub> + hydrocarbons	5.0-10.0

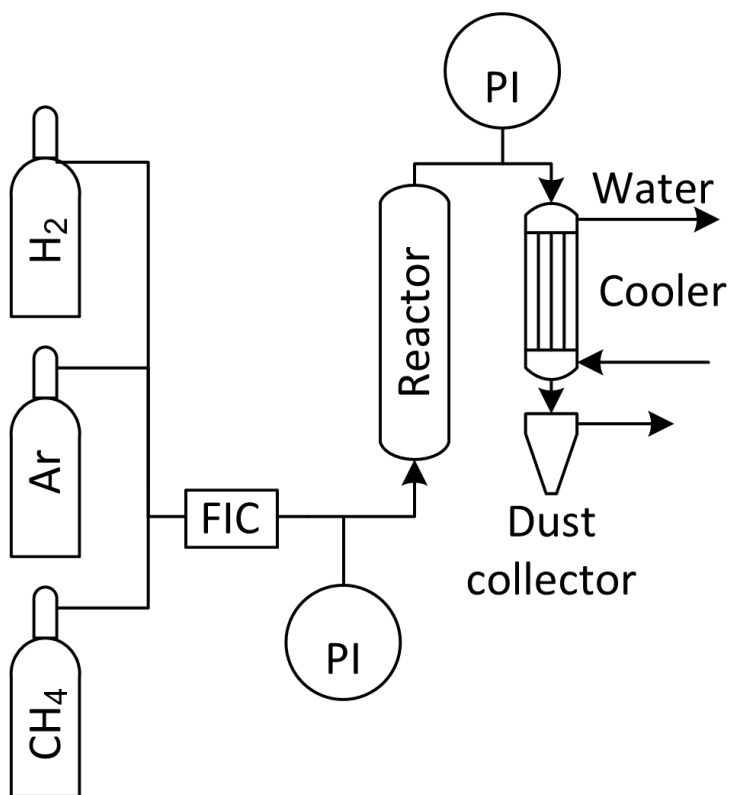


**Figure S1.** Flow diagram of the experimental unit

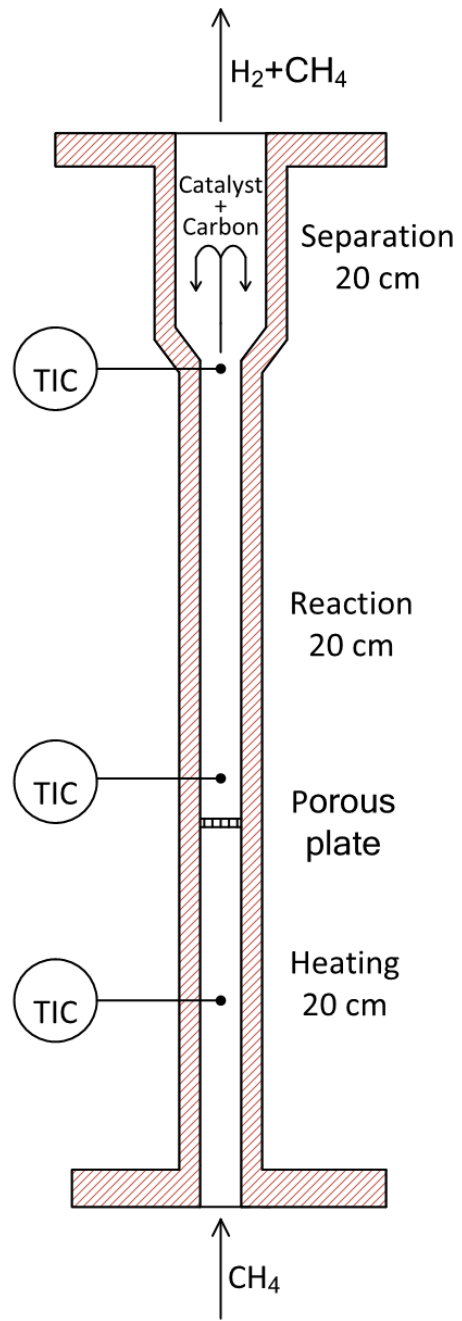
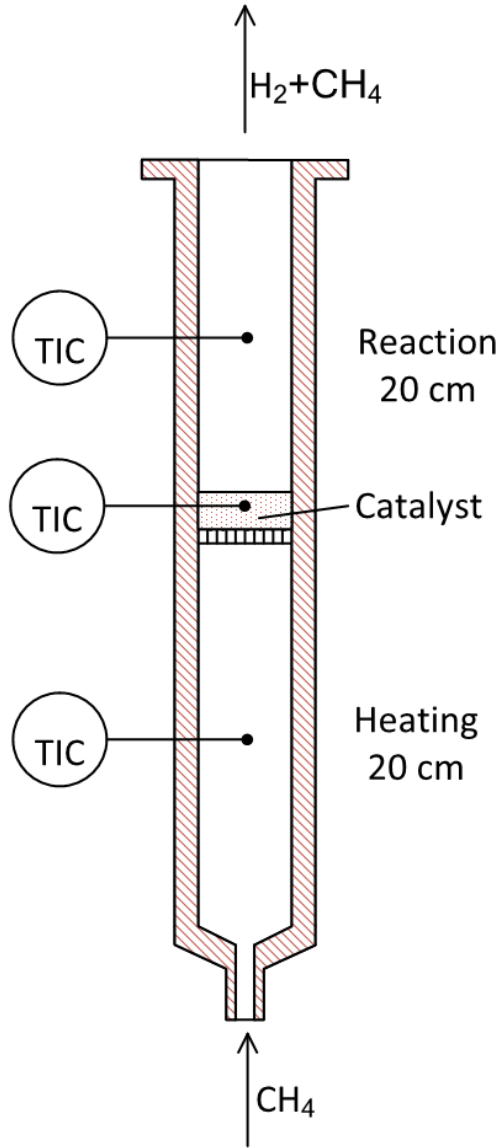


Figure S2. Fixed bed reactor used in the study.



**Figure S3.** Fluidized bed reactor used in the study.

### 3. Catalyst characterization

The synthesis of a catalyst was carried out by pH-controlled coprecipitation from solutions of metal nitrates with a total concentration of Mg, Al, and Ni cations of 1.0 mol/L. A solution of NaOH and Na<sub>2</sub>CO<sub>3</sub> with concentrations of 2.0 and 0.20 mol/L, respectively, was used as a precipitant. After coprecipitation, the precipitate was aged for 24 h. Then, the precipitate was washed and filtered under vacuum until the wash water reacted negatively to nitrate ions. The washed precipitate was dried at 100–120 °C to constant weight. Then, thermolysis of the resulting hydrotalcite was carried out at a temperature of 550 °C. In the second stage, the thermolysis products were placed into a Na<sub>2</sub>[Ni-EDTA] solution and kept for 10 h. The resulting Ni-EDTA precipitate was washed and filtered under vacuum until the wash water became colorless. The washed precipitate was dried at 100–120 °C to constant weight. The average particle size of the catalyst was 150–200 μm.

The X-ray diffraction pattern of a catalyst sample showed characteristic reflections of magnesium aluminium hydroxide carbonate hydrate  $2\theta=11.2; 22.4; 33.7; 38.7; 45.7$  (Table S2), magnesium aluminium hydroxide hydrate  $2\theta= 11.3; 22.8; 34.7; 39.1; 60.6; 61.9$  (Table S3) and jamborite  $2\theta=11.4; 22.9; 34.7; 39.0; 46.9; 60.2$  (Table S4). No individual phases of nickel or its oxides was detected. Probably, nickel in the catalyst was incorporated into the hydrotalcite structure. The resulting spinel phases had close lattice parameter values, and when X-ray diffraction patterns were taken, reflections from the planes of the phases merged into single diffraction peaks.

According to TGA-DSC data for the Ni-EDTA sample, the destruction of the sample occurred gradually. Water and several OH-groups released at 220 °C. The decomposition of EDTA occurred at 380–440 °C with the formation of layered structure intercalated with nickel. With a further increase in temperature up to 1050 °C, a gradual destruction of the layered structure of hydrotalcite occurred with the formation of nickel-aluminium spinel.

The BET isotherms of the catalyst were Type IV according to the IUPAC nomenclature; the presence of hysteresis indicated existence of mesopores in the sample. A large slope of the curve at small values of  $p/p_0$  indicated the presence of developed microporous structure. The specific area of the catalyst was 260 m<sup>2</sup>/g, and the average pore diameter was 4.5 nm.

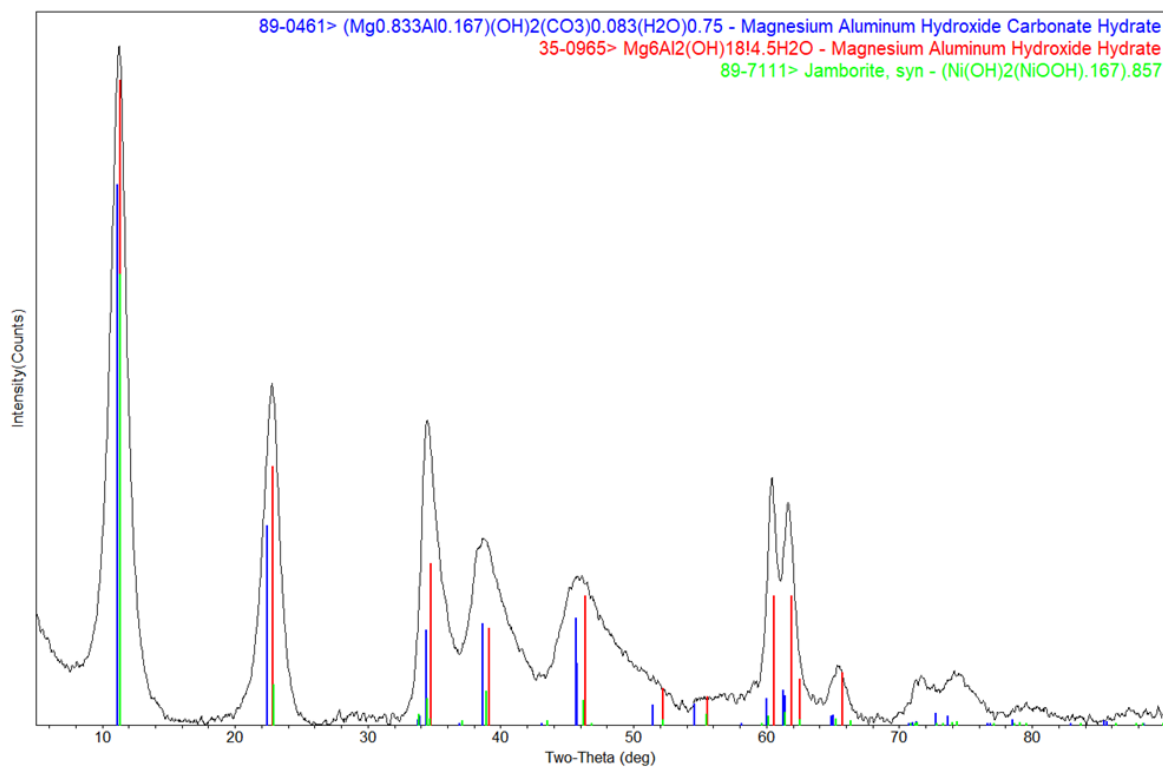


Figure S4. XRD pattern of the catalyst.

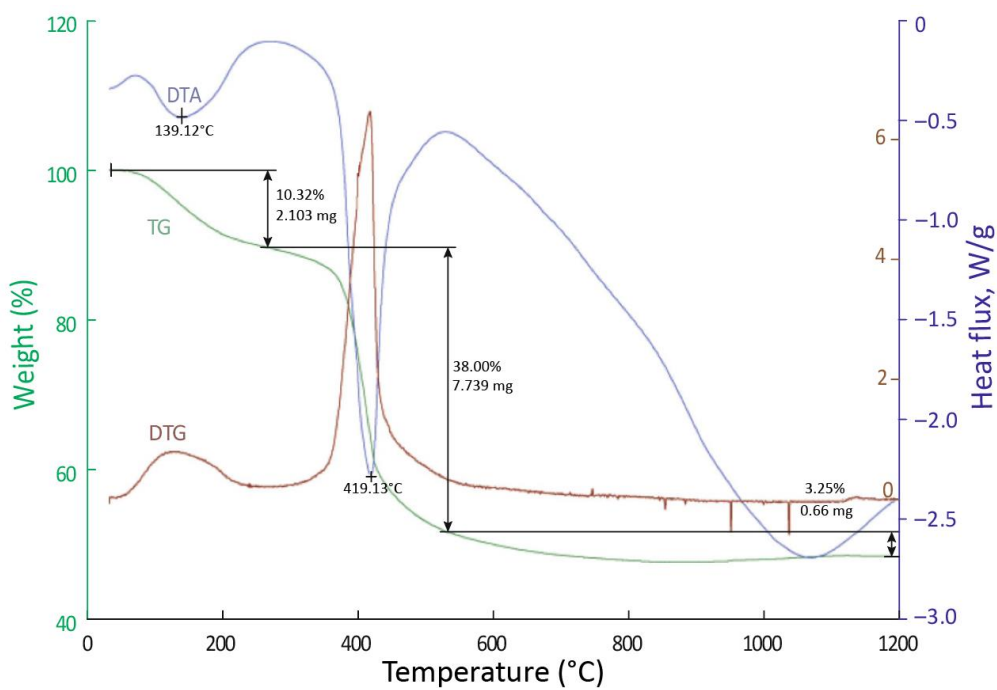


Figure S5. Differential thermal analysis curve of the catalyst.

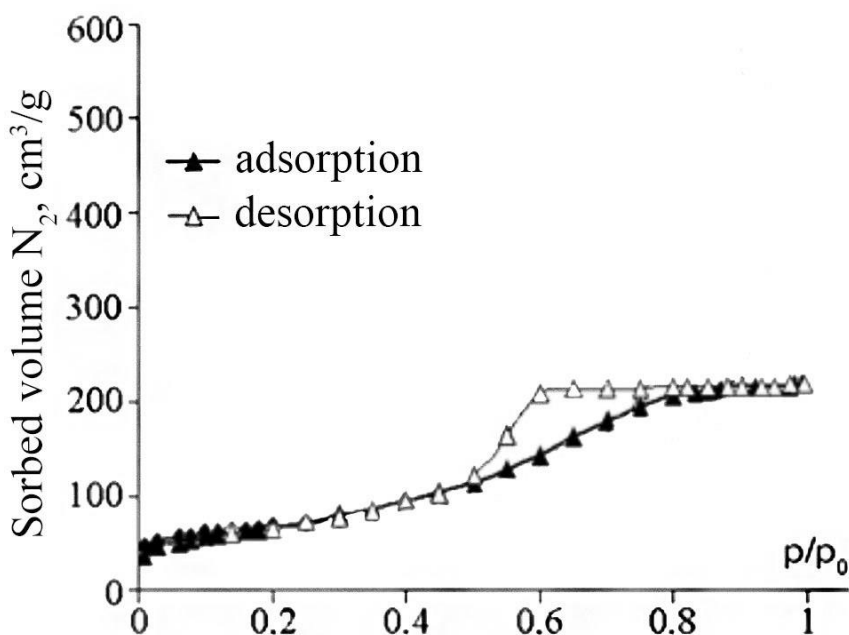


Figure S6. Nitrogen adsorption-desorption isotherms of the catalyst.

Table S2.

QM=Calculated(C); d=Calculated; l=Calculated													
Magnesium Aluminum Hydroxide Carbonate Hydrate ( Mg <sub>0.833</sub> Al <sub>0.167</sub> ) ( O H ) <sub>2</sub> ( C O <sub>3</sub> ) <sub>0.083</sub> ( H <sub>2</sub> O ) <sub>0.75</sub>													
Radiation=CuKα1 Calibration=						Lambda=1.540 Filter= l/lc(RIR)=2.34							
Ref: Calculated from ICSD using POWD-12++						60 2θ=11.151-88.401							
Rhombohedral - Powder Diffraction, R-3m (166) CELL: 3.0808 x 3.0808 x 23.784 <90.0 x 90.0 x 120.0>						Z=3 mp=		P.S.=hR7.58 (?)					
Density(c)=1.969 Density(m)=2.08A Mwt=77.26 Vol=195.50 Ref: Bellotto, M., Rebours, B., Clause, O., Lynch, J., Bazin, D., Elkaim, E.						F(30)=147.8(.0060,34/0)							
J. Phys. Chem., v100 p8527 (1996)													
FIZ=081964: X-ray diffraction (powder) Rietveld profile refinement applied ITF A reexamination of hydrotalcite crystal chemistry													
Strong Lines: 7.93/X 3.96/4 1.99/2 2.33/2 2.60/2 1.98/1 1.51/1 1.54/1 1.68/1 1.78/1													
33 Lines, Wavelength to Compute Theta = 1.54056A(Cu), I%-Type = Peak Height													
#	d(A)	I(f)	( h k l )	2-Theta	Theta	1/(2d)	#	d(A)	I(f)	( h k l )	2-Theta	Theta	1/(2d)
1	7.9280	100.0	( 0 0 3 )	11.151	5.576	0.0631	18	1.4330	1.7	( 0 1 14 )	65.030	32.515	0.3489
2	3.9640	36.8	( 0 0 6 )	22.410	11.205	0.1261	19	1.3308	0.2	( 1 1 9 )	70.733	35.366	0.3757
3	2.6514	0.8	( 1 0 1 )	33.778	16.889	0.1886	20	1.3308	0.2	( 0 2 1 )	70.733	35.366	0.3757
4	2.6427	1.6	( 0 0 9 )	33.893	16.946	0.1892	21	1.3257	0.4	( 2 0 2 )	71.046	35.523	0.3772

5	2.6033	17.6	(0 1 2)	34.421	17.210	0.1921	22	1.3213	0.5	(0 0 18)	71.318	35.659	0.3784
6	2.4342	0.1	(1 0 4)	36.895	18.448	0.2054	23	1.2986	2.2	(1 0 16)	72.766	36.383	0.3850
7	2.3270	18.7	(0 1 5)	38.661	19.331	0.2149	24	1.2845	1.6	(2 0 5)	73.695	36.847	0.3893
8	2.0984	0.1	(1 0 7)	43.071	21.536	0.2383	25	1.2417	0.1	(0 2 7)	76.679	38.340	0.4027
9	1.9857	19.7	(0 1 8)	45.650	22.825	0.2518	26	1.2390	0.1	(0 1 17)	76.877	38.439	0.4035
10	1.9820	11.2	(0 0 12)	45.740	22.870	0.2523	27	1.2171	0.9	(1 1 12)	78.525	39.263	0.4108
11	1.7754	3.5	(1 0 10)	51.426	25.713	0.2816	28	1.2171	0.9	(2 0 8)	78.525	39.263	0.4108
12	1.6798	3.9	(0 1 11)	54.587	27.293	0.2976	29	1.1635	0.2	(0 2 10)	82.911	41.455	0.4297
13	1.5856	0.1	(0 0 15)	58.129	29.065	0.3153	30	1.1353	0.7	(2 0 11)	85.448	42.724	0.4404
14	1.5404	4.8	(1 1 0)	60.007	30.003	0.3246	31	1.1333	0.6	(0 0 21)	85.641	42.820	0.4412
15	1.5121	6.4	(1 1 3)	61.248	30.624	0.3307	32	1.1333	0.6	(1 0 19)	85.641	42.820	0.4412
16	1.5089	5.3	(1 0 13)	61.394	30.697	0.3314	33	1.1049	0.1	(1 1 15)	88.401	44.201	0.4525
17	1.4358	1.5	(1 1 6)	64.889	32.444	0.3482							

Table S3.

<b>QM=Indexed(I); d=Guinier; I=Densitometer</b>													
Magnesium Aluminum Hydroxide Hydrate Mg <sub>6</sub> Al <sub>2</sub> (OH) <sub>18</sub> · 4.5 H <sub>2</sub> O													
Radiation=CuKα1 Calibration=Internal(PbNO <sub>3</sub> ) Ref: Lambda=1.540 Filter= I/Ic(RIR)= Mascolo, Marino. 4 2T=11.335- Mineral. Mag., v43 p619 (1980) 65.701													
Rhombohedral - (Unknown), R-3m (166) Z=0.375 mp= CELL: 3.054 x 3.054 x 23.4 <90.0 x 90.0 x 120.0> P.S=hR7.19 (?) Density(c)=1.930 Density(m)=1.990 Vol=189.01 F(11)=9.6(0.068,17/0) Mwt=586.99 Ref: Allmann. Chimia, v24 p99 (1970)													
NOTE: Hydrothermal treatment of MgO and alumina gel under CO <sub>2</sub> -free conditions. Sample dried on silica gel and contaminated with some brucite. Mascolo et al., Trans. J. Brit. Ceram. Soc., 79 6 (1980). Although much care was adopted to avoid the carbonation, the sample contains ~1% of CO <sub>2</sub> .													
Strong Lines: 7.80/X 3.89/4 2.58/3 1.96/2 1.53/2 1.50/2 2.30/2 1.65/1 1.75/1 1.42/1													
11 Lines, Wavelength to Compute Theta = 1.54056A(Cu), I%-Type = (Unknown)													
#	d(A)	I(f)	(h k l)	2-Theta	Theta	1/(2d)	#	d(A)	I(f)	(h k l)	2-Theta	Theta	1/(2d)
1	7.8000	100.0	(0 0 3)	11.335	5.667	0.0641	7	1.6530	9.0	(0 1 11)	27.774	13.887	0.3025
											55.549		
2	3.8900	40.0	(0 0 6)	22.842	11.421	0.1285	8	1.5270	20.0	(1 1 0)	60.588	30.294	0.3274
3	2.5800	25.0	(0 1 2)	34.742	17.371	0.1938	9	1.4980	20.0	(1 1 3)	61.889	30.944	0.3338
4	2.3000	15.0	(0 1 5)	39.133	19.567	0.2174	10	1.4850	7.0	(1 0 13)	31.246	15.623	0.3367



14	1.5355	1.8	( 1 1 0)	60.218	30.109	0.3256	31	1.1249	0.3	( 2 0 11)	86.436	43.218	0.4445
15	1.5061	2.8	( 1 1 3)	61.520	30.760	0.3320	32	1.1097	0.3	( 1 0 19)	87.917	43.959	0.4506
16	1.4819	1.0	( 1 0 13)	62.636	31.318	0.3374	33	1.1048	0.1	( 0 0 21)	88.412	44.206	0.4526
17	1.4271	1.3	( 1 1 6)	65.334	32.667	0.3504	34	1.0897	0.1	( 1 1 15)	89.963	44.982	0.4588

## 4. Analysis of the obtained carbon

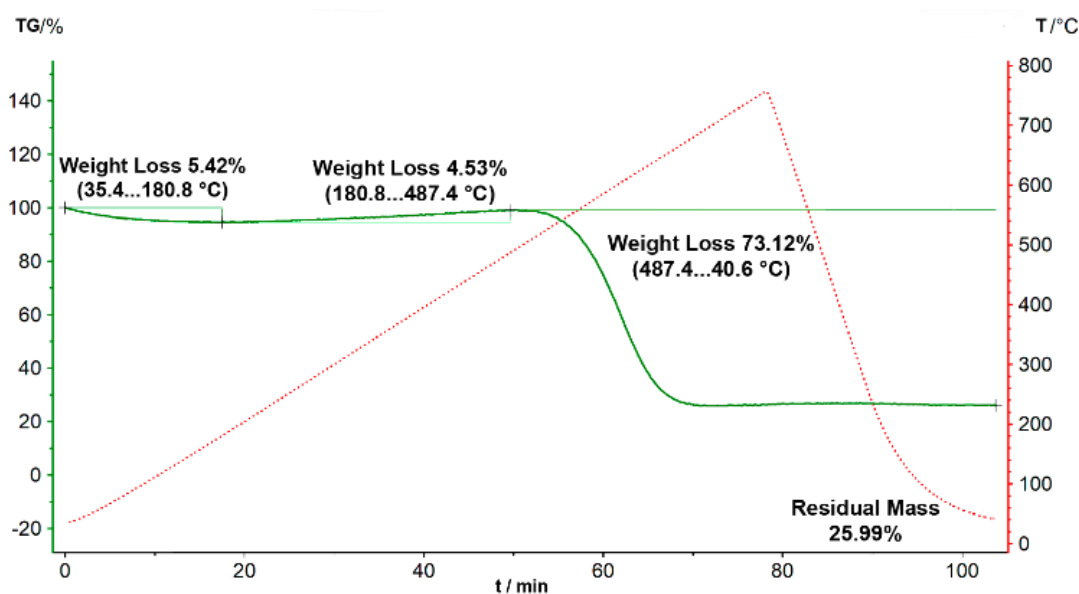


**Figure S7** Weight loss of a carbon sample under inert atmosphere (red curve shows the temperature program).

Probably, the first weight loss at 35–180 °C was due to evaporation of adsorbed water. Then, the oxidation of metals in the sample resulted in oxide formation and increased the weight (180–487 °C). Carbon oxidation started at 488 °C and finished at the maximum temperature program (820 °C) and remained the same under higher temperatures and cooling. The residual mass was 26%, so the carbon content was approximately 73%. The carbon content was high enough compared to other available sources of carbon.

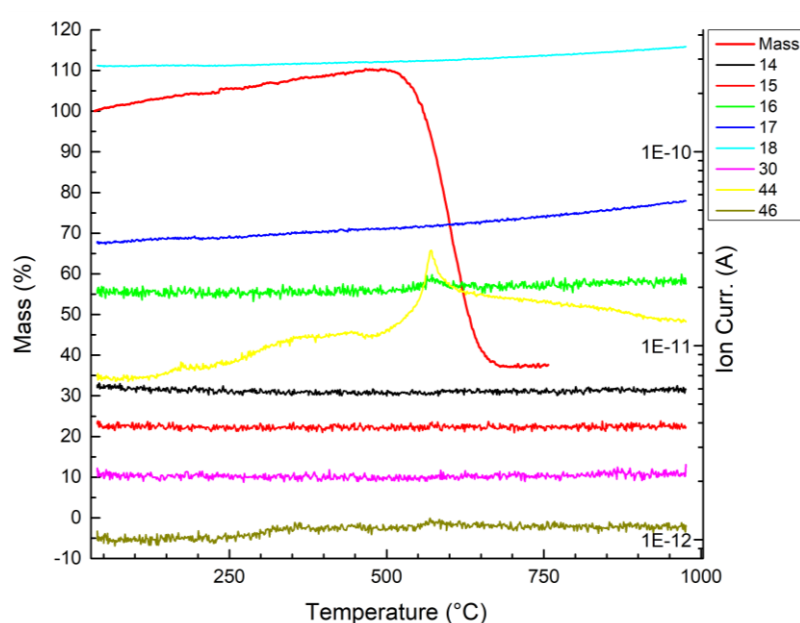


**Figure S8** Weight loss of a carbon sample under oxygen atmosphere detecting masses of products (upper red line is a weight loss line; the other coloured lines correspond to the MS-respond, and the masses of the products are given. CO<sub>2</sub> evolution after the oxidation process is reflected by the mass 44).

According to XRD analysis (Figure S9), the main component of the sample was graphite, and the impurities were iron oxides. Similar data were obtained using EDX analysis: some amounts of nickel and cobalt metals were present in a sample. According to SEM, the black powder contains micro-sized pieces of carbon (Figure S10).

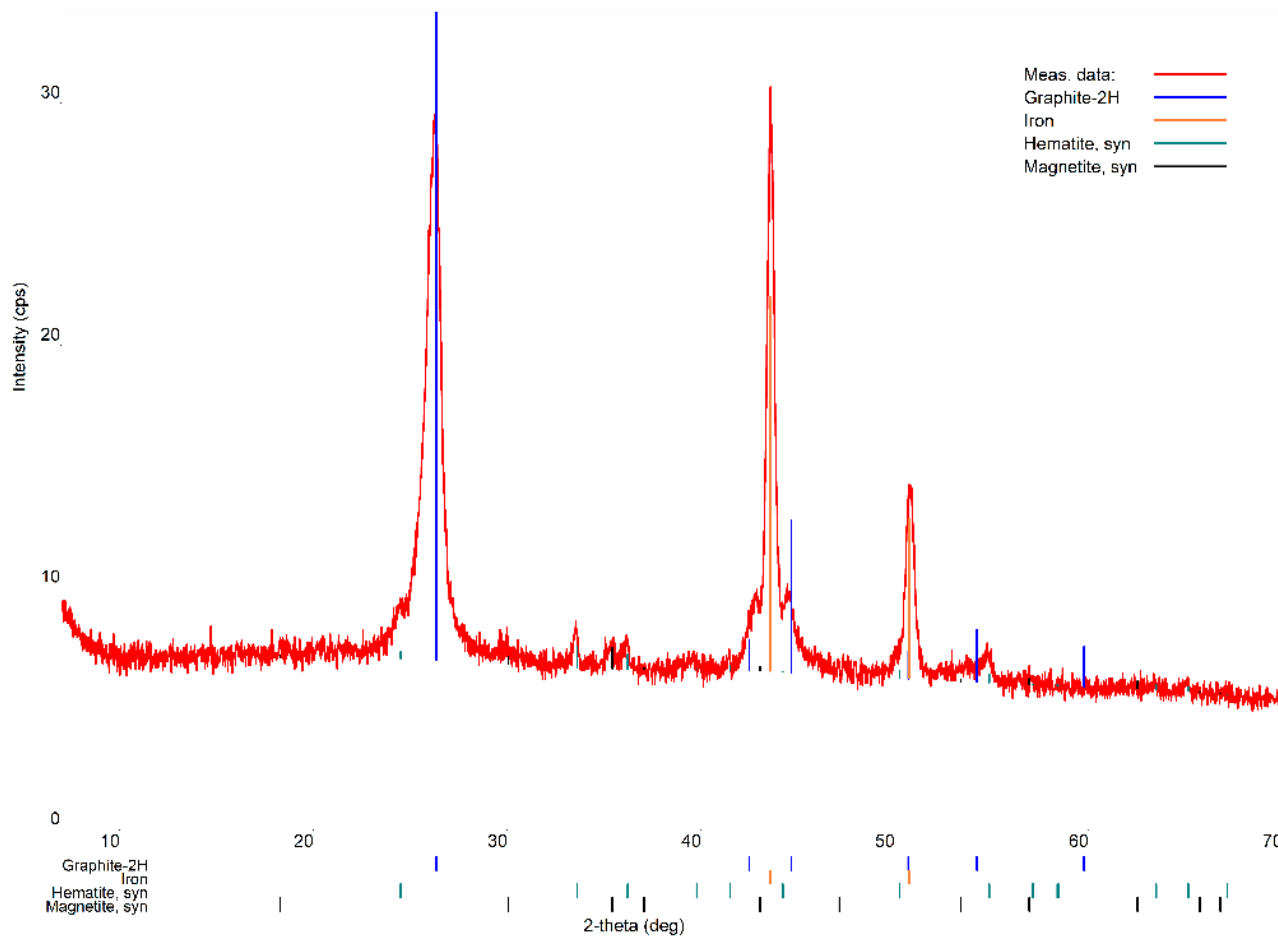


**Figure S9** XRD data for the obtained carbon sample. Lines: measurement data (red); graphite-2H (blue); iron (orange); hematite, syn (green); magnetite, syn (black).

Then, a sample of carbon (50.6 mg) was burnt in a crucible inside an oven at 900 °C for 2 hours to determine the nature of the residue. A total of 12.7 mg of a brown powder (25%) was obtained. The colour of the resulting powder was similar to the colour of the iron compounds. The brown powder was decomposed in an aliquot of concentrated nitric acid to convert metal into soluble nitrate forms. The residue was diluted with distilled water, centrifuged and analyzed by ICP compared with a blank sample of nitric acid treated as previously described. According to ICP analysis, the brown powder consisted of iron, nickel and cobalt compounds.

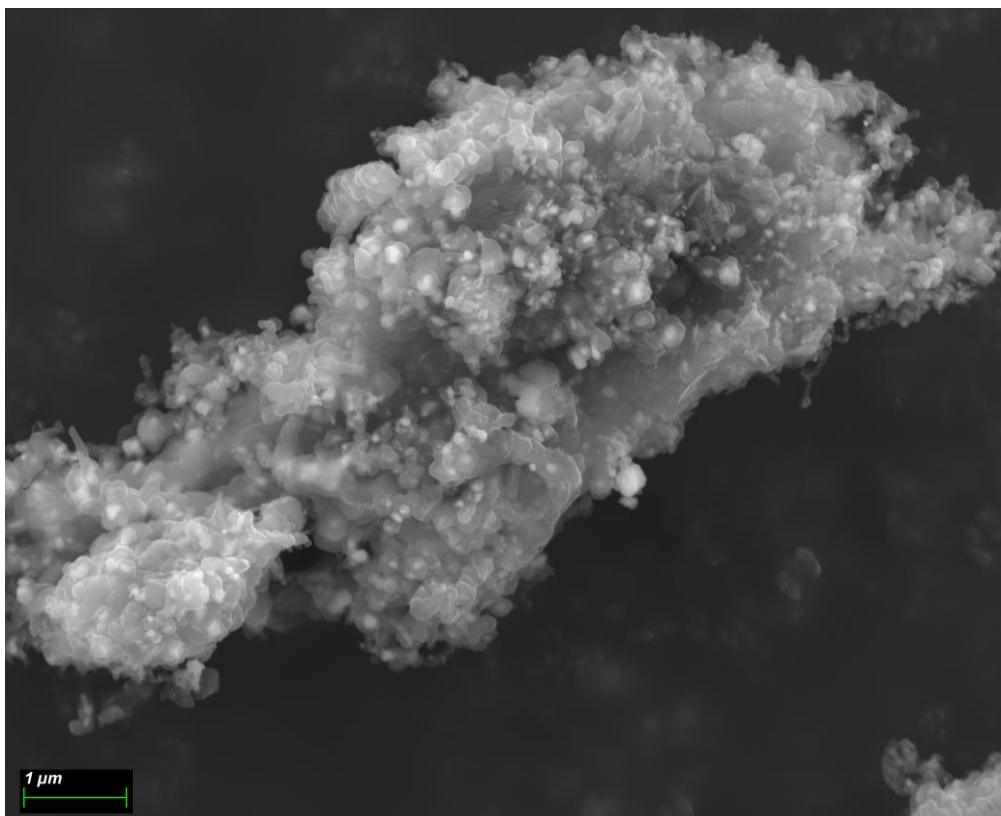


**Figure S10** SEM image of a sample of the obtained carbon.

#### **Preparation of calcium carbide**

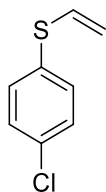
The obtained black powder was used as a carbon source for the synthesis of calcium carbide. Carbide was obtained from the product of pyrolysis and calcium metal melting the reaction mixture in an oven at 1100 °C for 1 h. The reaction occurred under vacuum in a quartz tube in a gram-scale loading. As a result, a grey highly reactive powder was obtained. First, a sample of carbide was treated with water in a capped vial. The released gas was taken with a syringe and injected into a gas chromatograph to identify acetylene. The only product in the chromatogram was acetylene, which had the same retention time as the gas from commercially available carbide. To evaluate the amount of acetylene, a sample of carbide was hydrolyzed with water, and the released gas was captured in a calibrated cylinder. A total of 1 mmol (64 mg) of the synthesized carbide generated 19.2 mL of the gaseous product. In a parallel experiment, 64 mg of commercially available carbide generated 19.8 mL of acetylene. In both cases, this corresponded to 75% carbide content in each sample.

## 5. NMR Spectra

The spectra are provided below to illustrate the purity of the obtained compounds.

### 4-Chlorophenyl vinyl sulfide

The compound was synthesized according to the procedure described elsewhere.<sup>[1]</sup>



$^1\text{H}$  NMR (400 MHz, DMSO)  $\delta$  7.48 – 7.42 (m, 1H), 7.41 – 7.35 (m, 1H), 6.71 (dd,  $J = 16.6, 9.6$  Hz, 1H), 5.43 (dd,  $J = 35.1, 13.1$  Hz, 1H).

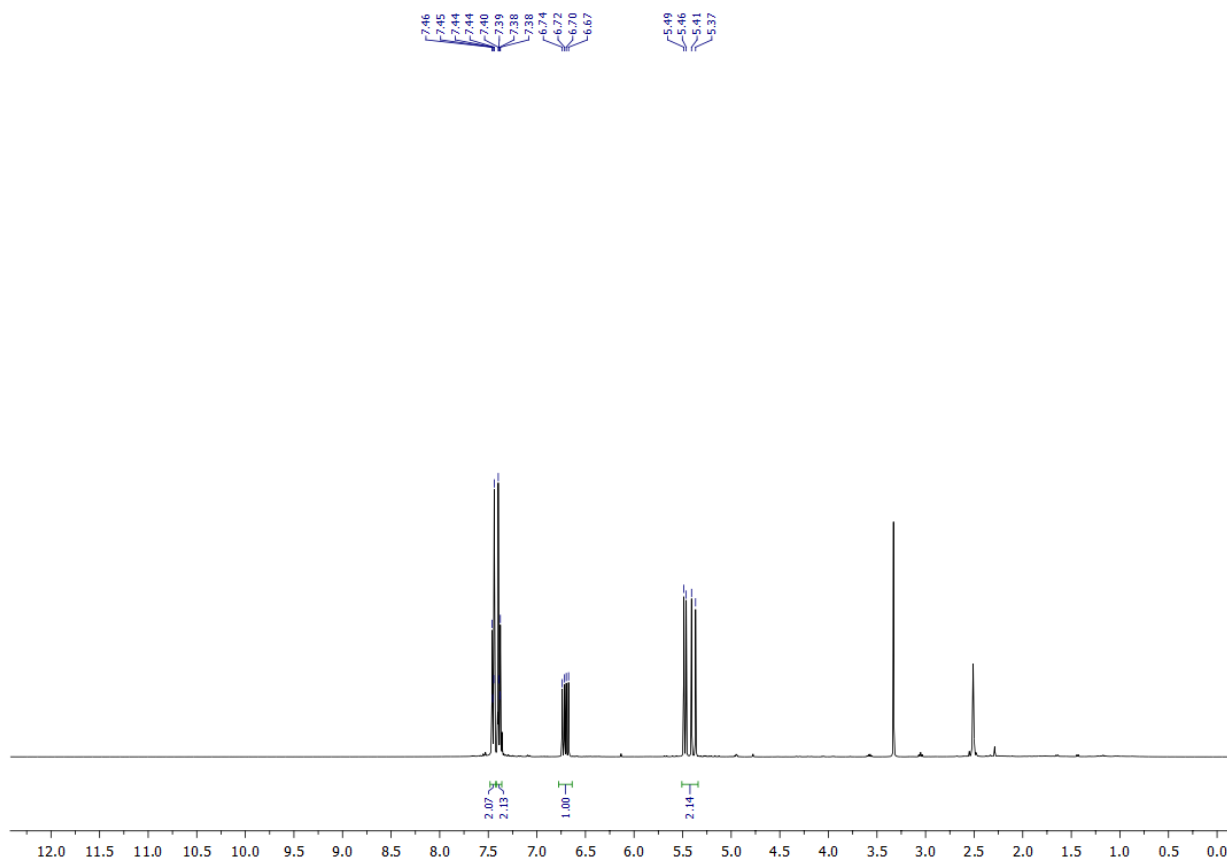
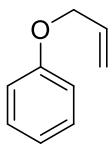


**Figure S11.**  $^1\text{H}$  NMR spectrum of 4-chlorophenyl vinyl sulfide (in DMSO- $d_6$ ).

## Benzyl vinyl ether

The compound was synthesized according to the procedure described elsewhere.<sup>[2]</sup>



<sup>1</sup>H NMR (400 MHz, DMSO)  $\delta$  7.47 – 7.28 (m, 1H), 6.60 (dd,  $J$  = 14.3, 6.8 Hz, 1H), 4.32 (dd,  $J$  = 14.2, 1.8 Hz, 1H), 4.06 (dd,  $J$  = 6.7, 1.8 Hz, 1H).

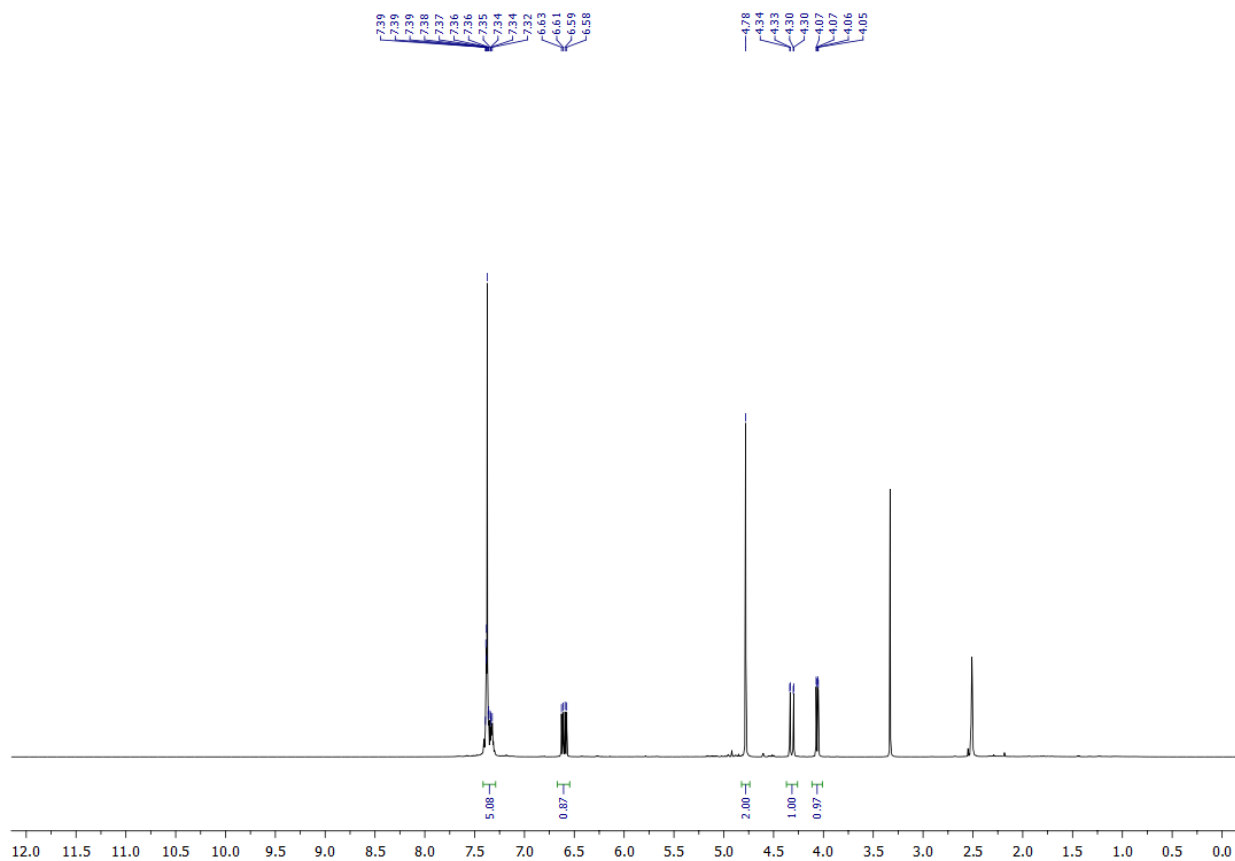
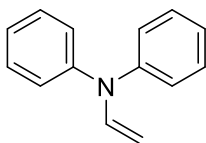


**Figure S12.** <sup>1</sup>H NMR spectrum of benzyl vinyl ether (in DMSO-d<sub>6</sub>).

### *N*-vinyl diphenyl amine

The compound was synthesized according to the procedure described elsewhere.<sup>[3]</sup>



<sup>1</sup>H NMR (400 MHz, DMSO) δ 7.40 – 7.31 (m, 4H), 7.15 – 7.08 (m, 3H), 7.08 – 7.03 (m, 1H), 7.03 – 6.98 (m, 4H), 4.09 (d, *J* = 8.6 Hz, 1H), 3.82 (d, *J* = 15.1 Hz, 1H).

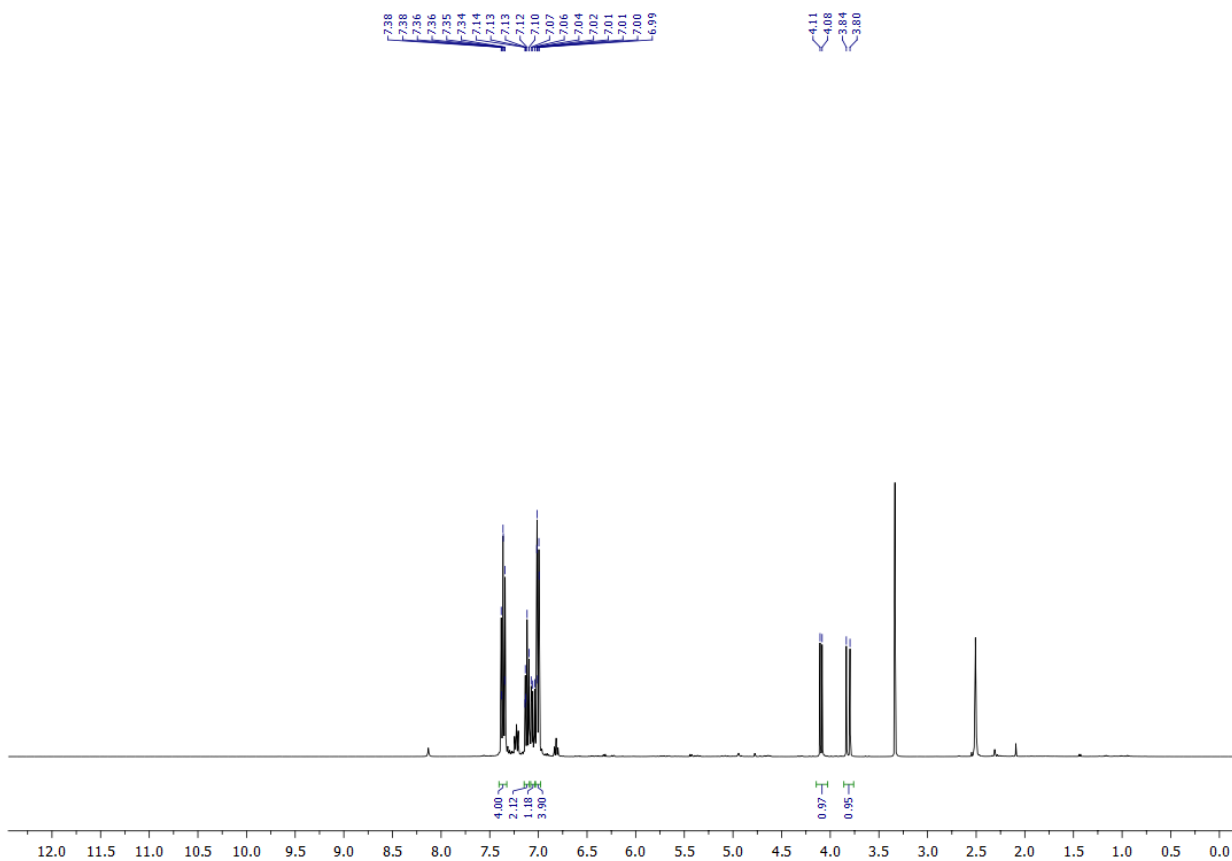
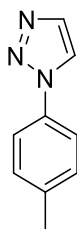


**Figure S13.** <sup>1</sup>H NMR spectrum of *N*-vinyl diphenyl amine (in DMSO-*d*<sub>6</sub>).

## 4-Tolyltriazole

The compound was synthesized according to the procedure described elsewhere.<sup>[4]</sup>



<sup>1</sup>H NMR (400 MHz, CDCl<sub>3</sub>) δ 7.98 (s, 1H), 7.84 (s, 1H), 7.62 (d, *J* = 8.4 Hz, 2H), 7.32 (d, *J* = 8.2 Hz, 2H), 2.42 (s, 3H).

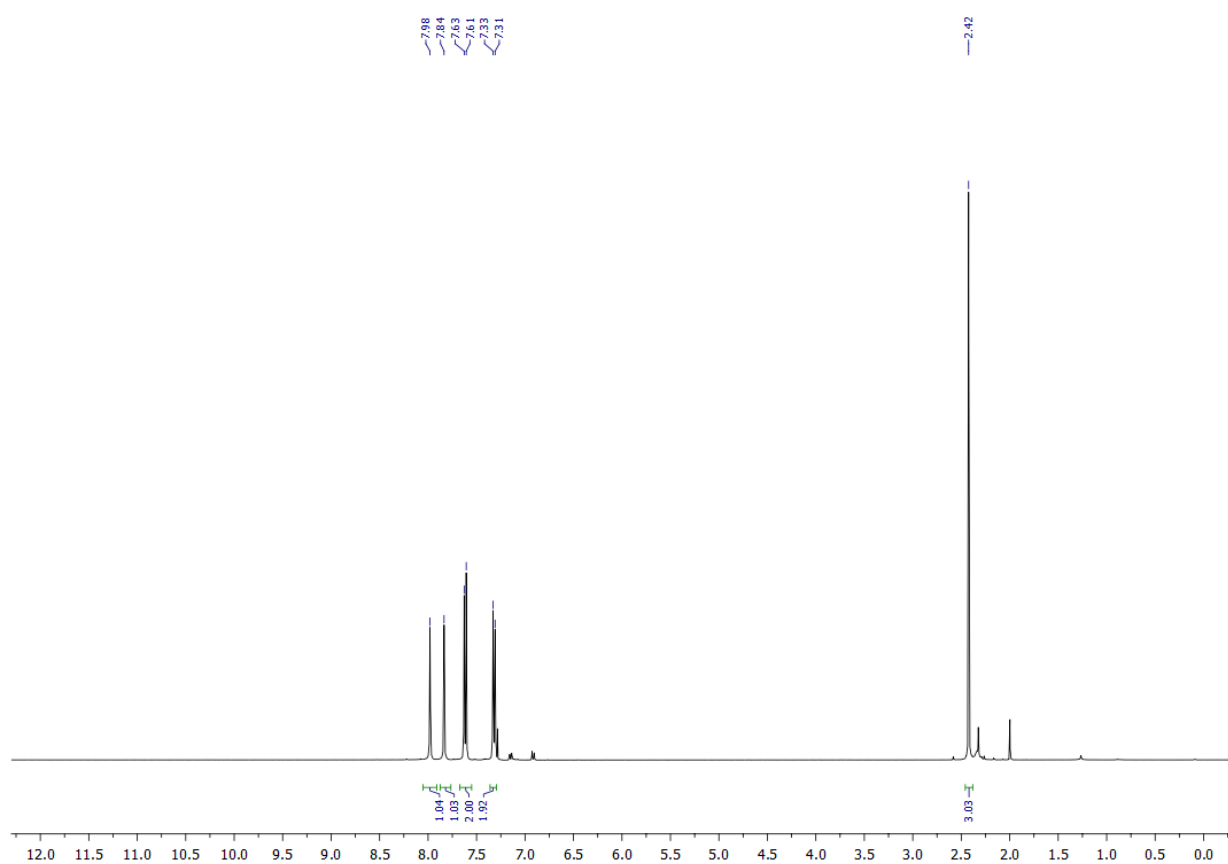


**Figure S14.** <sup>1</sup>H NMR spectrum of 4-tolyltriazole (in DMSO-d<sub>6</sub>).

## 6. EDX analysis of carbon sample.

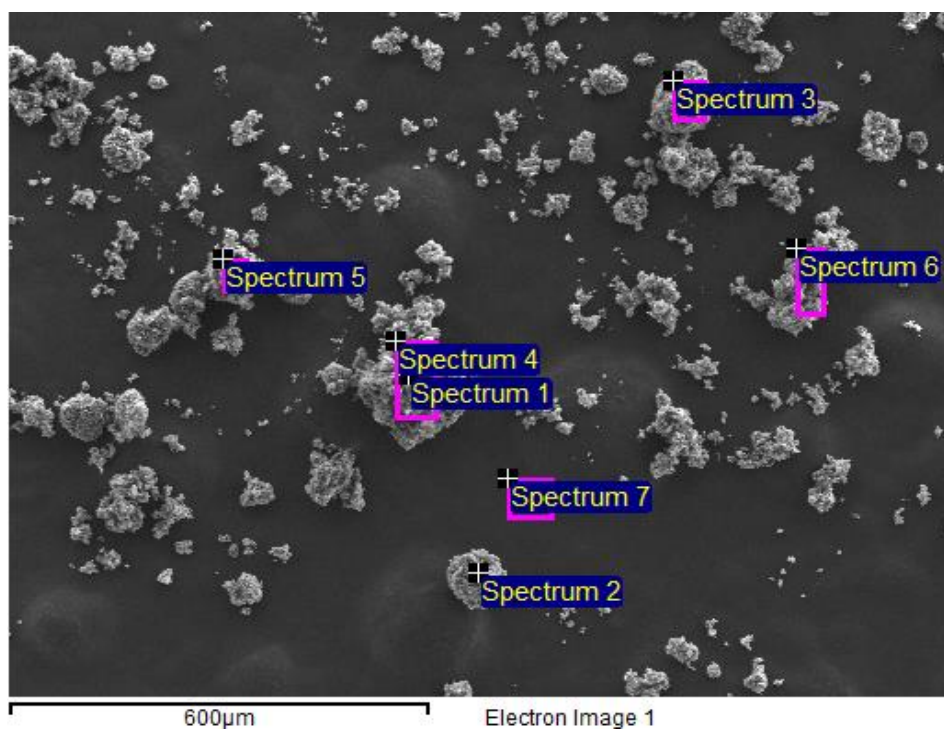


**Figure S15.** EDX analysis of the carbon sample after methane cracking. Total view.

Table S4. The composition of carbon sample. Processing option: All elements analysed (Normalised). All results in weight%

Spectrum	In stats.	C	O	Si	Cr	Fe	Ni	Total
Spectrum 1	Yes	81.97	1.12		1.60	8.33	6.97	100.00
Spectrum 2	Yes	89.51		0.52	0.88	6.76	2.33	100.00
Spectrum 3	Yes	88.69	1.52		1.10	5.61	3.07	100.00
Spectrum 4	Yes	82.94	2.04	0.35	1.87	8.27	4.52	100.00
Spectrum 5	Yes	86.39	2.26	0.38	1.29	6.16	3.52	100.00
Spectrum 6	Yes	82.11	2.22	0.36	1.58	7.91	5.81	100.00
Spectrum 7	Yes	82.42	17.58					100.00
Max.		89.51	17.58	0.52	1.87	8.33	6.97	
Min.		81.97	1.12	0.35	0.88	5.61	2.33	

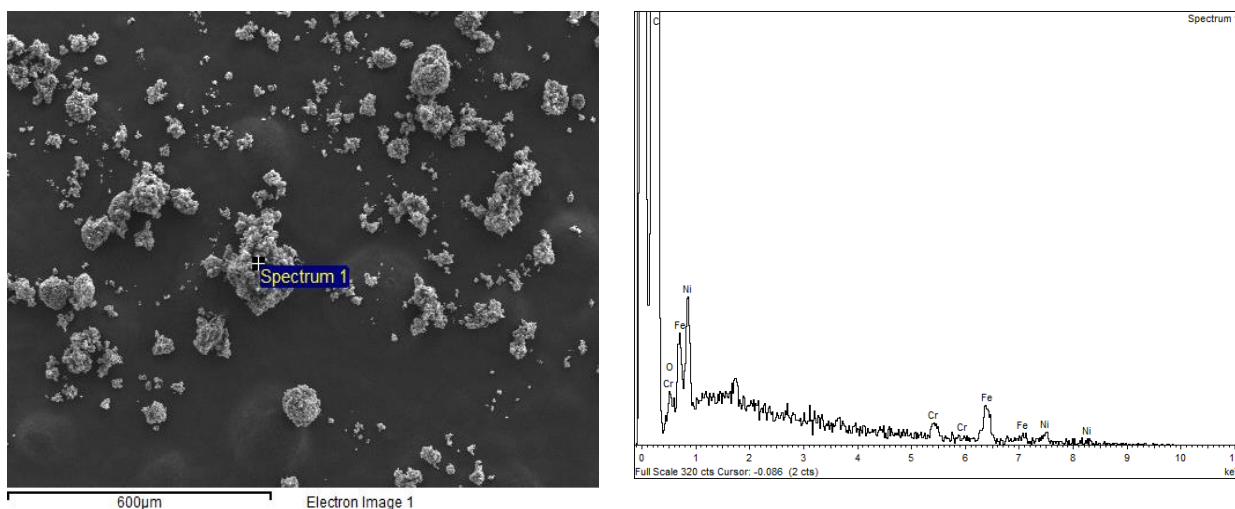


Figure S16. EDX data for the carbon sample. Selected area – Spectrum 1.

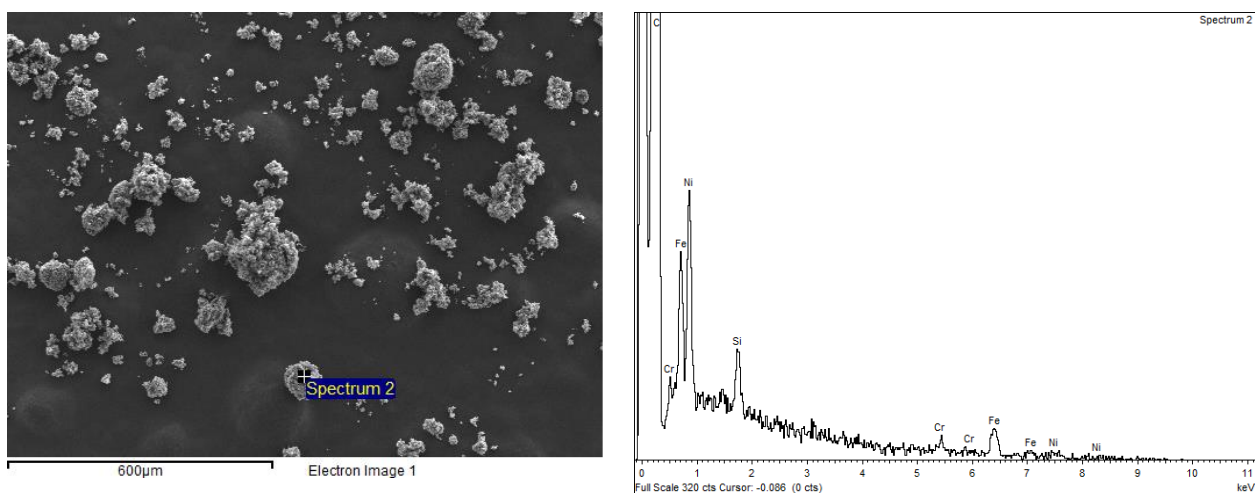


Figure S17. EDX data for the carbon sample. Selected area – Spectrum 2.

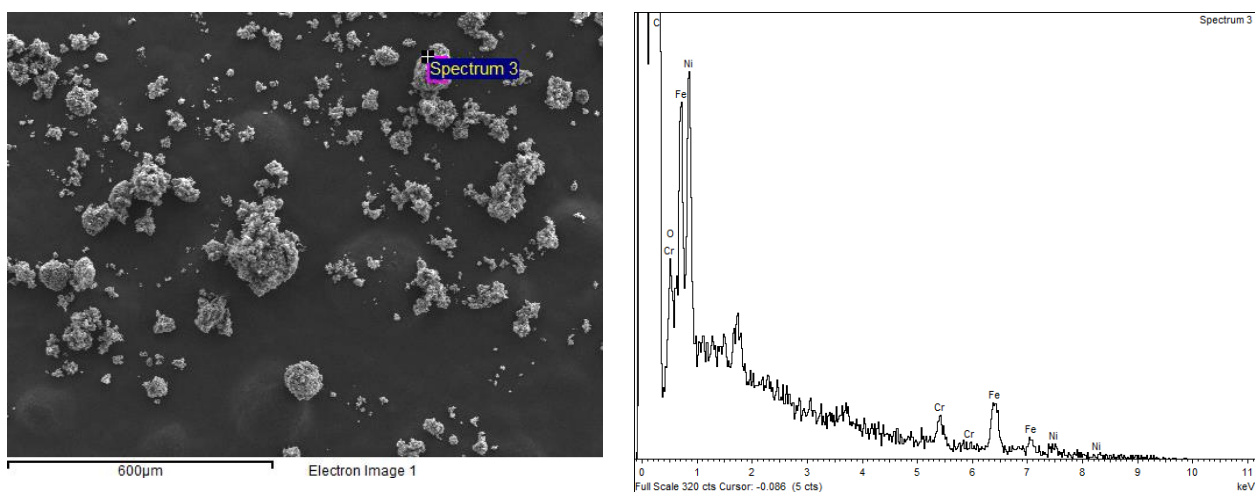


Figure S18. EDX data for the carbon sample. Selected area – Spectrum 3.

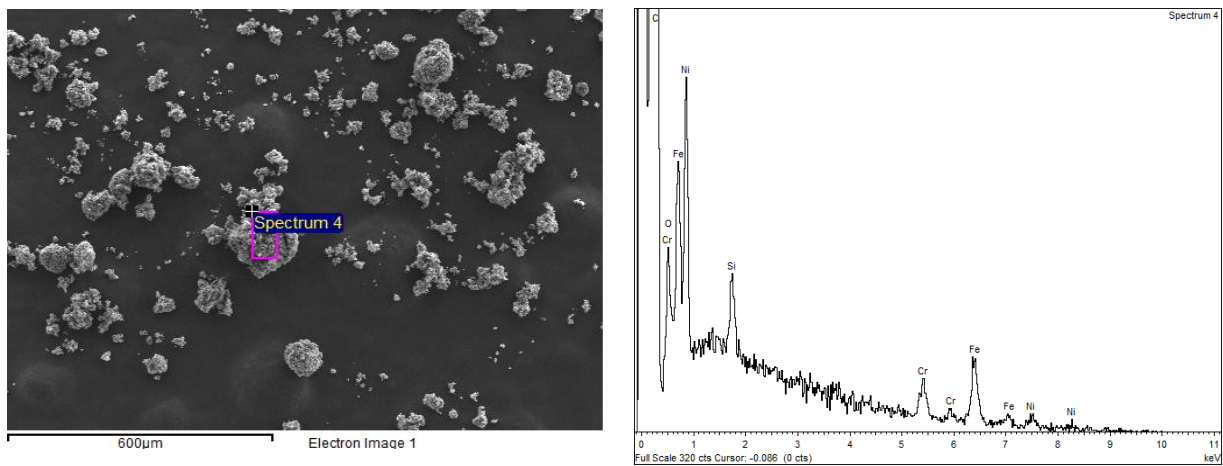


Figure S19. EDX data for the carbon sample. Selected area – Spectrum 4.

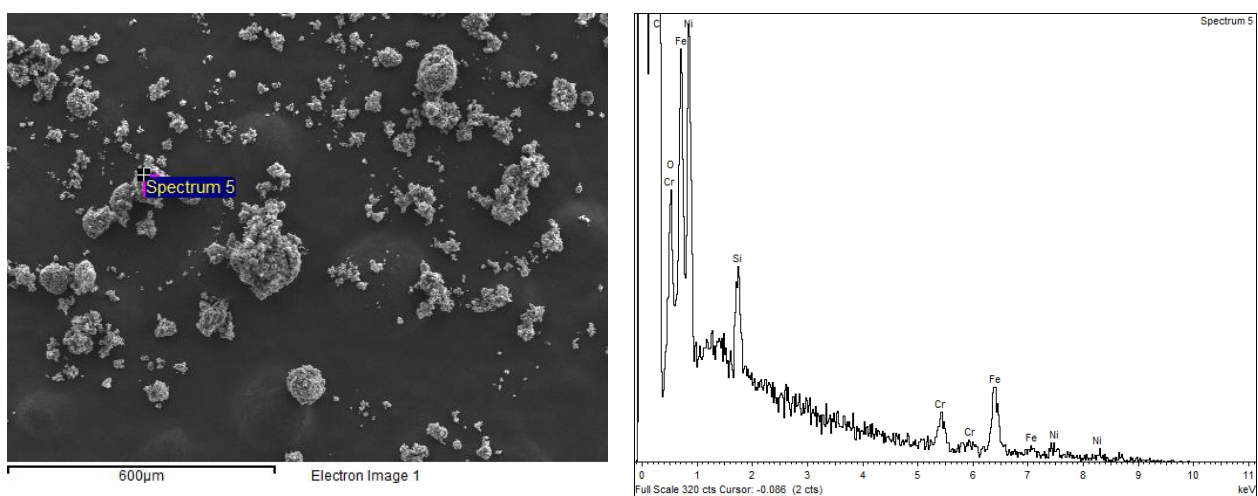


Figure S20. EDX data for the carbon sample. Selected area – Spectrum 5.

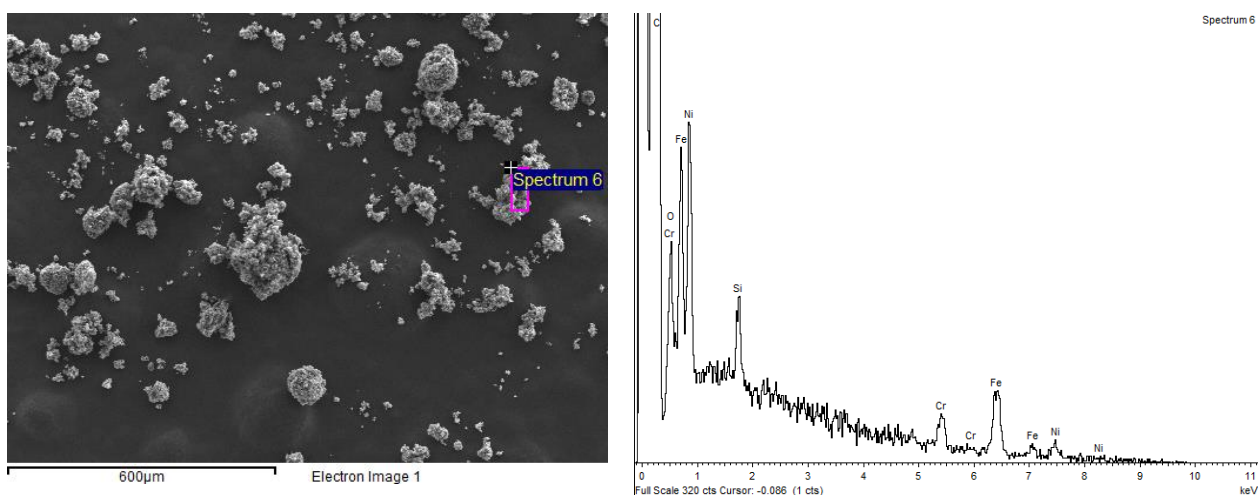
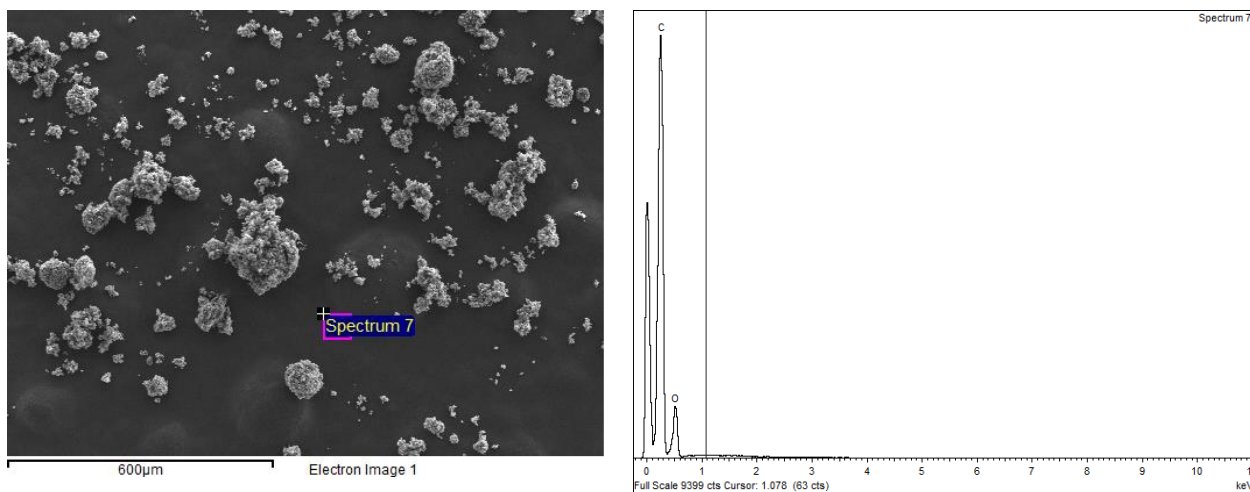
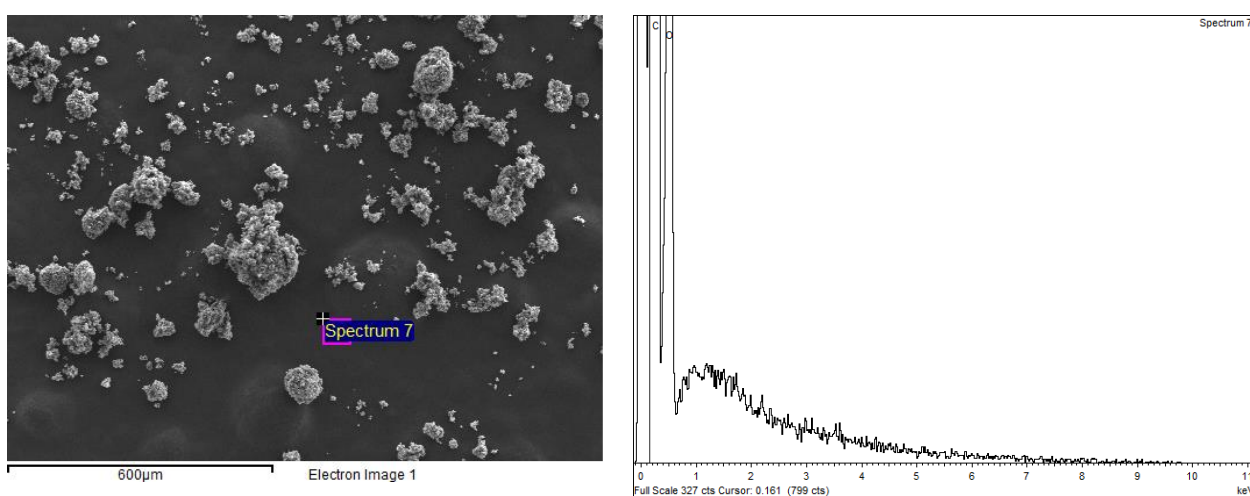


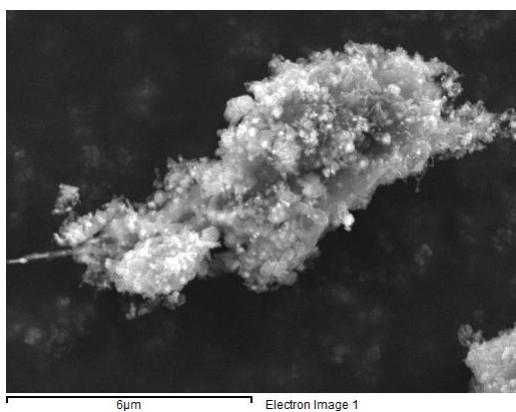
Figure S21. EDX data for the carbon sample. Selected area – Spectrum 6.



**Figure S22.** EDX data for the carbon sample. Selected area – Spectrum 7.



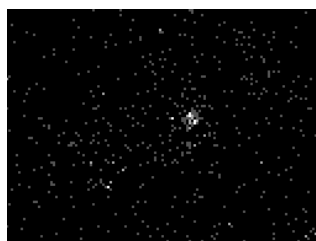
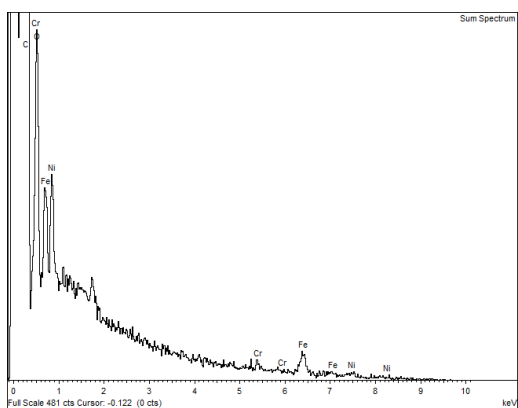
**Figure S23.** EDX data for the carbon sample. Selected area – Spectrum 7.



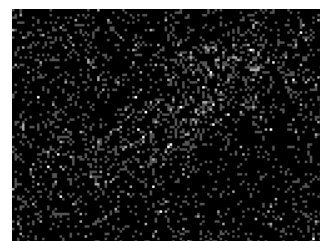
C Ka1\_2



O Ka1



Cr Ka1

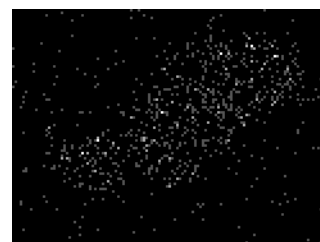


Si Ka1

Spectrum	C	O	Cr	Fe	Ni
Sum Spectrum	92.72	4.03	0.29	2.01	0.95
Mean	92.72	4.03	0.29	2.01	0.95
Std. deviation	0.00	0.00	0.00	0.00	0.00
Max.	92.72	4.03	0.29	2.01	0.95
Min.	92.72	4.03	0.29	2.01	0.95



Ni Ka1



Fe Ka1

**Figure S24.** EDX map of a carbon sample after methane cracking.

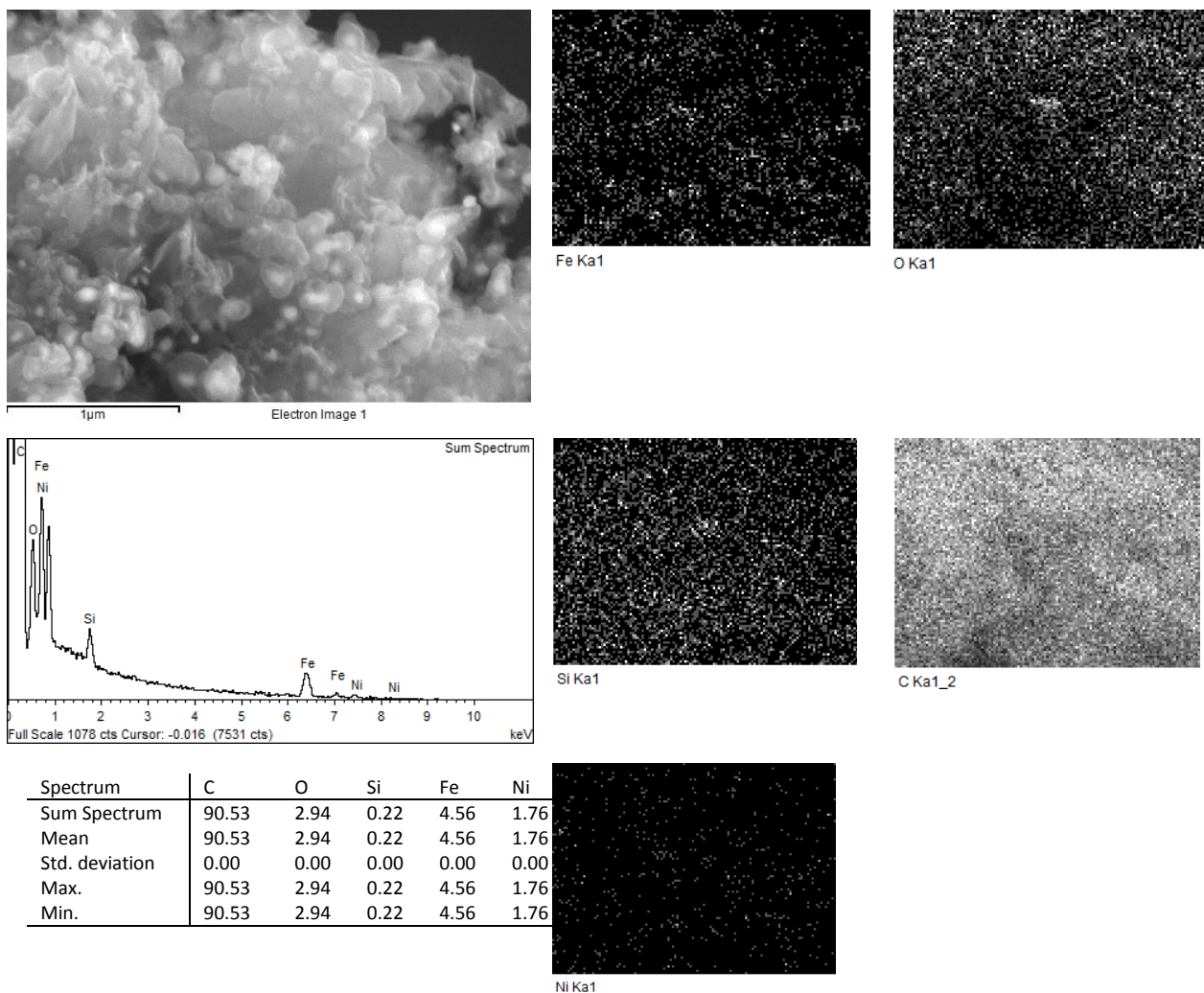


Figure S25. EDX map of a carbon sample after methane cracking.

## 7. ICP data

ICP element analysis

Method of atomic emission spectrometry with inductively coupled plasma ICPE-9000

No	Run	Ba			Ca			Cd			Co			Cr					
		$\lambda=455,403$ nm			$\lambda=186,801$ nm			$\lambda=214,438$ nm			$\lambda=228,616$ nm			$\lambda=205,552$ nm					
		LQ=0,001 mg/L			LQ=0,03mg/L			LQ=0,002 mg/L			LQ=0,001 mg/L			LQ=0,004 mg/L					
		C $\pm$ $\Delta$ , mg/L		RS D, %	C $\pm$ $\Delta$ , mg/L		RS D, %	C $\pm$ $\Delta$ , mg/L		RS D, %	C $\pm$ $\Delta$ , mg/L		RS D, %	C $\pm$ $\Delta$ , mg/L		RS D, %			
1	Blank	0,049	$\pm$	0,011	5	19,6	$\pm$	4,2	5	<LQ		0,004	$\pm$	0,001	6	0,456	$\pm$	0,020	1
2	Sample	0,039	$\pm$	0,008	5	16,4	$\pm$	3,5	5	<LQ		0,019	$\pm$	0,002	2	2,210	$\pm$	0,190	2

No	Run	Cu			Fe			K			Mg			Mn							
		$\lambda=213,590$ nm			$\lambda=259,940$ nm			$\lambda=769,896$ nm			$\lambda=285,213$ nm			$\lambda=260,569$ nm							
		LQ=0,008mg/L			LQ=0,001 mg/L			LQ=0,03mg/L			LQ=0,001 mg/L			LQ=0,001 mg/l							
		C $\pm$ $\Delta$ , mg/L		RS D, %	C $\pm$ $\Delta$ , mg/L		RS D, %	C $\pm$ $\Delta$ , mg/L		RS D, %	C $\pm$ $\Delta$ , mg/L		RS D, %	C $\pm$ $\Delta$ , mg/L		RS D, %					
1	Blank	<LQ			2,58	$\pm$	0,11	1	0,454	$\pm$	0,039	2	2,88	$\pm$	0,12	1	0,071	$\pm$	0,003	1	
2	Sample	0,065	$\pm$	0,006	2	9,29	$\pm$	0,80	2	0,212	$\pm$	0,018	2	2,47	$\pm$	0,53	5	0,236	$\pm$	0,010	1

No	Run	Na			Ni			Pb			V			Zn			
		$\lambda=588,592$ nm			$\lambda=231,604$ nm			$\lambda=216,99$ nm			$\lambda=292,402$ nm			$\lambda=206,200$ nm			
		LQ=0,003 mg/L			LQ=0,003 mg/L			LQ=0,01 mg/L			LQ=0,003 mg/L			LQ=0,002mg/L			
		C $\pm$ $\Delta$ , mg/L		RS D, %	C $\pm$ $\Delta$ , mg/L		RS D, %	C $\pm$ $\Delta$ , mg/L		RS D, %	C $\pm$ $\Delta$ , mg/L		RS D, %	C $\pm$ $\Delta$ , mg/L		RS D, %	
1	Blank	1,79	$\pm$	0,08	1	0,25	$\pm$	0,01	1	<LQ		<LQ		0,09	$\pm$	0,00	1

					9		1					5		4			
2	Sample	1,59	±	0,14	2	2,92	±	0,25	2	<LQ		<LQ		0,069	±	0,006	2

Standards for each element for calibration were prepared from a multicomponent calibration standard MERC in 0.1N HNO<sub>3</sub>. The range of the solution was 0.001-100 mg/L. Analysis of the solutions was performed in axial mode without dilution. All the samples were filtered through "Blue tape" filter.

## References.

- [1] K. S. Rodygin, V. P. Ananikov, "An efficient metal-free pathway to vinyl thioesters with calcium carbide as the acetylene source" *Green Chem.* **2016**, *18*, 482.
- [2] G. Werner, K. S. Rodygin, A. A. Kostin, E. G. Gordeev, A. S. Kashin, V. P. Ananikov, "A solid acetylene reagent with enhanced reactivity: fluoride-mediated functionalization of alcohols and phenols" *Green Chem.* **2017**, *19*, 3032.
- [3] K. S. Rodygin, A. S. Bogachenkov, V. P. Ananikov, "Vinylolation of a secondary amine core with calcium carbide for efficient post-modification and access to polymeric materials" *Molecules* **2018**, *23*, 648.
- [4] V. V. Voronin, M. S. Ledovskaya, K. S. Rodygin, V. P. Ananikov, "Cycloaddition reactions of *in situ* generated C<sub>2</sub>D<sub>2</sub> in dioxane: efficient synthetic approach to D<sub>2</sub>-labeled nitrogen heterocycles" *Eur. J. Org. Chem.* **2021**, *2021*, 5640.